

Reaction $^{40}\text{Ca}(e, e'p)$ and Observation of the $1s$ Proton State*

K. Nakamura, S. Hiramatsu, T. Kamae, and H. Muramatsu†
Department of Physics, University of Tokyo, Bunkyo-ku, Tokyo, Japan

and

N. Izutsu
*Kéage Laboratory of Nuclear Science, Institute for Chemical Research,
 Kyoto University, Sakyo-ku, Kyoto, Japan*

and

Y. Watase‡
Department of Physics, Niigata University, Igarashi, Niigata, Japan
 (Received 22 July 1974)

The distorted spectral function of the protons in the reaction $^{40}\text{Ca}(e, e'p)$ is measured. For the $2s$ - $1d$ region the distorted-wave impulse-approximation calculation using the Elton-Swift wave functions explains the data within 20%. The $1p$ occupation number is 1.7 times that of the shell-model prediction. After correcting for the radiative effects and for the multiple-collision background the $1s$ state is clearly observed at $E_s \approx 58$ MeV with a reasonable occupation number.

Separation energies of deeply bound nuclear protons give the vital information to the theory of nuclear matter. Does the separation energy for the most deeply bound $1s$ protons increase as the nuclear mass number A increases? Or does the nuclear binding saturate at a certain binding energy? In this regard the $1s$ separation energy of ^{40}Ca has attracted much attention¹⁻⁵ in recent years. The experimental methods employed by these groups¹⁻⁵ are the high-energy quasifree scatterings,⁶ namely $(p, 2p)$ or $(e, e'p)$ reactions. Generally speaking the $(e, e'p)$ process is considered to be an ideal means of studying deeply bound protons, whereas the $(p, 2p)$ process suffers badly from very strong distortion effects due to nuclear interaction.⁶ Despite continuing efforts no conclusive evidence of observing the $1s$ proton state has been reported and thus this problem still remains unanswered.

Amaldi *et al.*¹ have observed a peak in the $^{40}\text{Ca}(e, e'p)$ cross section at $E_s = 77 \pm 14$ MeV which they believe corresponds to removal of $1s$ -shell protons. The evidence, however, is poor since the momentum distribution has not been measured and since the statistics are insufficient. James *et al.*⁴ and Kullander *et al.*⁵ have observed a peak in the $(p, 2p)$ cross section at $E_s \sim 50$ MeV which they believe corresponds to the $1s$ -shell proton removal. However, a severe complication in the analysis of $(p, 2p)$ data arises from consideration of the multiple-collision process which forms a large background with respect to

the direct $1s$ knock-out process. The analysis of Kullander *et al.*⁵ in the distorted-wave impulse approximation (DWIA) shows that the experimental $1s$ occupation number is about 100 times greater than the shell-model prediction. This clearly indicates that unless the background processes are understood to an accuracy of a few percent, the claimed peak cannot be taken as the real signal of the $1s$ state.

We present here the distorted spectral function of the protons in the reaction⁷ $^{40}\text{Ca}(e, e'p)$ and show conclusive evidence of the $1s$ proton state by properly taking into consideration the radiative corrections and the multiple-collision background. The experiment was performed at the Institute for Nuclear Study, University of Tokyo. An electron beam of 700–750 MeV primary energy was used with a natural calcium target (~ 200 mg/cm²). The scattered electrons were momentum analyzed by a magnetic spectrometer and the knocked-out protons were detected by a range spark chamber. Since our apparatus had an acceptance of 60 MeV for the proton separation energy, three independent measurements with different kinematical conditions were made to cover the E_s range up to 130 MeV. We call these measurements runs I, II, and III, as the measured E_s interval increases. The radiative corrections⁸ were applied only to run I. The data obtained in the other runs were not corrected for the radiative effects. This is because we were able to measure only the data in a limited E_s interval in

each kinematical condition, and for runs II and III the data of the smaller E_S sides taken under the same kinematical conditions were needed to unfold the radiative tail. Further description of the experiment is given elsewhere.⁷

Figure 1 shows the E_S dependence of the distorted spectral function $Q(E_S, p_0)$ integrated over the momentum intervals indicated:

$$A(E_S) = 4\pi \int p_0^2 Q(E_S, p_0) dp_0,$$

where p_0 is the momentum of the proton bound in the nucleus; the definition of $Q(E_S, p_0)$ is given by Hiramatsu *et al.*⁹ The error bars show the statistical error only. The systematic normalization error is estimated to be about 10%. To see the general structure of the separation-energy spectrum in Fig. 1 we normalize the data of run I to that of run II by a normalization factor 0.56.¹⁰

We can see an indication of several shell-model single-particle contributions in Fig. 1. However, to obtain quantitative information, we rely on a phenomenological fit to the data of run I by the expression in the DWIA:

$$Q(E_S, p_0) = \sum_{nlj} C_{nlj} A_{nlj}(E_S) \rho_{nlj}(p_0).$$

Here $A_{nlj}(E_S)$ is the energy distribution function (normalized to the shell-model occupation num-

ber), and $\rho_{nlj}(p_0)$ is the distorted momentum distribution due to the removal of the protons in the (nlj) shell. The adjustable parameter C_{nlj} represents the extent to which the DWIA accounts for the data (it should be around unity if the DWIA correctly accounts for the data). The functional form of $A_{nlj}(E_S)$ is taken as a Gaussian with two adjustable parameters: width and peak energy (note: the width includes the experimental energy resolution, ~ 7 MeV). The distorted momentum distribution $\rho_{nlj}(p_0)$ is calculated in the WKB approximation⁶ using the Elton-Swift single-particle wave function¹¹ for the bound proton and the optical potential given by Kerman, McManus, and Thaler¹² with a Fermi-type form factor for the knocked-out proton. The result of the χ^2 minimization fit is tabulated in Table I and is shown by the solid curves *a* in Fig. 1. The features of the fit are as follows:

(1) The states $1d_{3/2}$, $2s_{1/2}$, and $1d_{5/2}$ are well fitted and the resulting C_{nlj} 's are consistent with the shell model to within about 20%.

(2) The states $1p_{1/2}$ and $1p_{3/2}$ cannot be separated, and are combined as a single $1p$ state. Its occupation number is 1.7 times that of the shell-model prediction.

(3) The $1s$ state contributes as a broad continuous background in the run-I range, and thus the best-fit parameters are not unique. This is rather natural since the E_S range measured in run I hardly covers the $1s$ region. The dashed curves in Fig. 1 show, for comparison, the calculation with the normal shell-model occupation numbers (i.e., $C_{nlj} = 1$) for all the states except for the $1s$ state ($C_{1s} = 0$).

To obtain detailed information on the $1s$ state, we now turn our attention to the analysis of run II. We assume that the measured cross section in run II consists of an incoherent sum of the true $1s$ contribution, the contribution from the upper shells including the radiative effects,⁸ and the

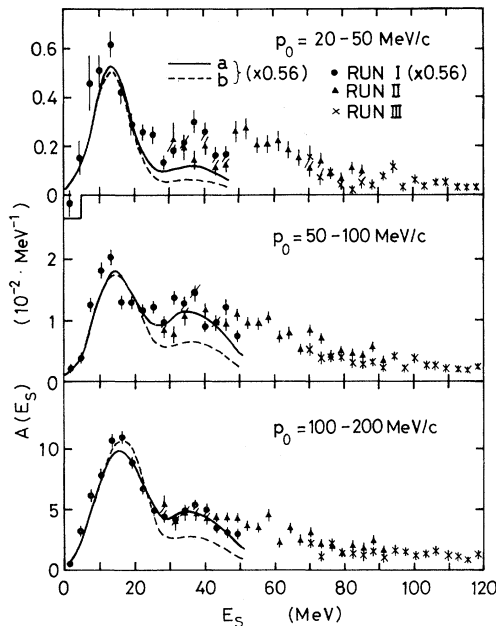


FIG. 1. Distorted spectral function integrated over p_0 . Superimposed curves are DWIA calculation for $2s$, $1d$, and $1p$ using Elton-Swift wave functions with parameters given in Table I (solid curves *a*) and with shell-model occupation numbers (dashed curves *b*).

TABLE I. Parameters for the solid curves *a* in Fig. 1 ($1d_{3/2}$, $2s_{1/2}$, $1d_{5/2}$, and $1p$ states) and for the dot-dashed curves in Fig. 2 ($1s$ state).

State	C_{nlj}	Peak energy (MeV)	Width (FWHM) (MeV)
$1d_{3/2}$	1.04 ± 0.40	10.4 ± 1.4	9.2 ± 1.3
$2s_{1/2}$	1.02 ± 0.06	13.6 ± 0.4	12.0 ± 0.9
$1d_{5/2}$	0.78 ± 0.26	18.4 ± 1.6	9.9 ± 1.4
$1p$	1.70 ± 0.15	35.3 ± 0.5	23.5 ± 2.3
$1s$	1.87 ± 0.09	58.4 ± 1.1	31.9 ± 1.1

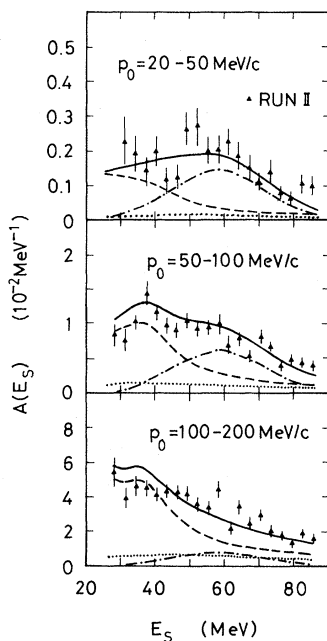


FIG. 2. Data obtained in run II. Superimposed curves are radiative ($e, e'p$) cross section (dashed curves) and multiple collision background (dotted curves); $1s$ contribution (dot-dashed curves); sum of all the contributions (solid curves).

background due to the multiple-collision process.⁹ The last two are in principle calculable if we know the spectral function in the lower E_S region. For the calculation of the radiative tail we took the distorted spectral function used in the calculation of the dashed curves in Fig. 1. The multiple-collision contribution to the cross section was calculated using a Monte Carlo technique. These results are shown in Fig. 2 by the dashed (radiative) and dotted (multiple) curves. Since these curves do not include the $1s$ contribution, the difference between the data and the calculated curve is due to the $1s$ proton removal and was fitted by the $1s$ wave function of Elton and Swift.¹¹ The result is shown by the dot-dashed curves in Fig. 2 and the parameters obtained are listed in the last line of Table I. Although there may still exist ambiguity in the choice of the spectral function, the important facts are (1) the extensive calculations on the radiative cross section and on the multiple-collision background do not show any enhancement or any structure as functions of E_S or p_0 at separation energies around $E_S = 58$ MeV; (2) the momentum distribution in the rele-

vant E_S region is consistent with the s -wave state⁷; (3) the occupation number of the $1s$ state calculated from our data is consistent with the shell-model prediction within a factor of 2—not a factor of 100 as in the ($p, 2p$) results. Thus we conclude that the enhancement of the data centered at $E_S \sim 58$ MeV is, in fact, due to the removal of $1s$ state protons.

We gratefully acknowledge the cooperation and assistance of the Institute for Nuclear Studies synchrotron crew and the Institute for Nuclear Studies high-energy group. We also thank Dr. S. Kullander, Dr. J. Mougey, Dr. E. De Sanctis, Dr. L. R. B. Elton, Dr. N. Austern, and Dr. S. Pittel for communicating their works.

*Work supported in part by the Grant-in-Aid from the Ministry of Education.

†Present address: Software Division, Fujitsu Limited, Ohta-ku, Tokyo, Japan.

‡Present address: National Laboratory for High Energy Physics, Oho-machi, Tsukuba, Ibaraki, Japan.

¹U. Amaldi, Jr., *et al.*, Phys. Lett. **22**, 593 (1966).

²G. Campos Venuti *et al.*, Nucl. Phys. **A205**, 628 (1973).

³A. Bussiere *et al.*, Lett. Nuovo Cimento **2**, 1149 (1971).

⁴A. N. James *et al.*, Nucl. Phys. **A138**, 145 (1969).

⁵G. Landaud *et al.*, Nucl. Phys. **A173**, 337 (1971); S. Kullander *et al.*, Nucl. Phys. **A173**, 357 (1971).

⁶G. Jacob and Th. A. J. Maris, Rev. Mod. Phys. **38**, 121 (1966), and **45**, 6 (1973).

⁷K. Nakamura, thesis, University of Tokyo, 1973 (unpublished).

⁸E. Borie and D. Drechsel, Nucl. Phys. **A167**, 369 (1971).

⁹S. Hiramatsu *et al.*, Phys. Lett. **44B**, 50 (1973).

¹⁰The normalization factor 0.56 is introduced only to make the continuation from run I to run II in the separation-energy spectra look smooth to show the general structure of the separation-energy spectra in the entire E_S range. In the subsequent analysis the absolute values of the cross sections are used and this normalization factor is not used. The difference in the normalization between runs I and II in their overlap region is due mainly to (1) the data of run I is radiatively corrected while that of run II is not; (2) the distorted spectral function has dependence on the kinematical conditions which are different between runs I and II.

¹¹L. R. B. Elton and A. Swift, Nucl. Phys. **A94**, 52 (1967).

¹²A. K. Kerman, H. McManus, and R. M. Thaler, Ann. Phys. (New York) **8**, 551 (1959).